Journal of Solid State Chemistry 183 (2010) 262–269

Contents lists available at ScienceDirect

Journal of Solid State Chemistry

journal homepage: www.elsevier.com/locate/jssc

The influence of sulfur substitution on the atomic displacement in $Bi_2Ti_2O_7$

Beverly Brooks Hinojosa, Paul M. Lang, Aravind Asthagiri *

Department of Chemical Engineering, University of Florida, Gainesville, FL 32611, USA

ARTICLE INFO

Article history:
Received 9 May 2009
Received in revised form
30 October 2009
Accepted 9 November 2009
Available online 13 November 2009

Keywords:
Cubic pyrochlore
Density functional theory
Bismuth titanate
Bismuth ruthenate
Lattice disorder

ABSTRACT

To clarify the role of A_2O' and B_2O_6 networks on cation displacement observed in $Bi_2Ti_2O'O_6$, we used density functional theory calculations to examine the effect of sulfur substitution on the O′ and O sites on lone pair formation and resulting atomic displacement observed in $Bi_2Ti_2O'O_6$. Cation displacement in bismuth titanate is suppressed only when S is substituted on the O′ site. Analysis of the electronic structure shows that S substitution on the O′ site suppresses the formation of the asymmetric p-type lone pair by modifying the Bi-anion hybridization. Lone pair formation is favored in $Bi_2Ti_2O'S_6$ and the atomic displacement is larger than that observed in $Bi_2Ti_2O'O_6$. This enhanced displacement is due to weaker Bi–S versus Bi–O interactions leading to significantly stronger hybridization between the Bi and O′ states in $Bi_2Ti_2O'S_6$. We also induced lone pair formation in a metallic bismuth pyrochlore oxide ($Bi_2Ru_2O'O_6$) by modifying the Bi–O interactions through S substitution on the B_2O_6 network, indicating atomic displacement on the A_2O' network may be achieved by modifying the B_2O_6 network.

1. Introduction

Bismuth based pyrochlores, such as $(Bi_{1.5}Zn_{0.42})(Zn_{0.5}Nb_{1.5})O_{6.92}$ (BZN), have garnered much attention recently due to their high dielectric permittivity, low loss and tunable temperature coefficient of capacitance [1–3]. The pyrochlore oxide, with molecular formula $A_2B_2O_7$, is often thought of as the two interpenetrating networks A_2O' and B_2O_6 (see Fig. 1) consisting of corner sharing A_4O' tetrahedrons and BO_6 octahedrons [4]. The dielectric properties of these materials are often attributed to ion hopping of A and O′ atoms [1], but open questions remain to the extent of substitutional disorder [2] on the A_2O' network (Fig. 1a) versus the B_2O_6 network (Fig. 1b) influence on the ion hopping in these systems [3]. A general feature observed in all the Bi pyrochlores that show high dielectric permittivity is large ion displacement from the ideal $Fd\bar{3}m$ sites of the cubic pyrochlore structure. This atomic displacement results in multiple energetically equivalent sites that facilitate cation hopping. Because compounds such as BZN incorporate cation substitutions onto both the A_2O' and B_2O_6 networks it is difficult to fully separate the myriad of influences on cation displacement. In order to overcome this difficulty, we recently investigated a series of cubic bismuth pyrochlores without cation substitution ($Bi_2B_2O_6O'$, *B*=Ti, Ru, Rh, Os, Ir, Pt) using density functional theory (DFT) [5]. Only $Bi_2Ti_2O_7$ showed a preference for atomic displacement and the magnitude from DFT matched the experimentally reported values [6,7]. Through the analysis of the electronic structure of $Bi_2Ti_2O'O_6$, the atomic displacement was attributed to the development of a lone pair on the Bi cations. The lone pair does not form for the other bismuth pyrochlores examined confirming that the B_2O_6 network has some influence in the lone pair formation. In this contribution, we further develop the role of the B_2O_6 versus A_2O' network in the formation of the lone pair in $Bi_2Ti_2O'O_6$ by examining the effect of sulfur substitution on the two networks.

Walsh and co-workers showed that substitution of sulfur for oxygen suppressed the formation of the lone pair observed in PbO [8–10]. This suppression of the lone pair explains the difference in structure between PbO (litharge) and PbS (rocksalt). More importantly, the work on PbO and PbS shows that the lone pair formation is dependent on the cation–anion hybridization and not just due to hybridization of 6*s* and 6*p* orbitals of Pb [8]. In our earlier study, we showed that the B_2O_6 network influences lone pair formation in Bi pyrochlores through a secondary effect. For the semi-metallic and metallic systems the Bi cations interact more strongly with the O anions within the B_2O_6 network. This stronger Bi–O interactions weakens the Bi–O′ interactions, which in turn suppresses the formation of the lone pair. This model for lone pair formation essentially matches the conclusion from DFT studies of lead oxides and bismuth oxides by Walsh et al. [8–11]. Specifically, in lead oxides and bismuth oxides the nature of the cation–anion direct bonding is critical to induce lone pair formation, but in pyrochlores the B_2O_6 network can influence the primary Bi–O′ interactions.

In this paper, we employ a similar approach to Walsh and co-workers to further elucidate the lone pair formation in $Bi_2Ti_2O'O_6$ through sulfur substitution. Though some pyrochlore compounds

* Corresponding author. Fax: +1 352 392 9513.
E-mail address: aasthagiri@che.ufl.edu (A. Asthagiri).

0022-4596/$ - see front matter © 2009 Elsevier Inc. All rights reserved.
doi:10.1016/j.jssc.2009.11.010

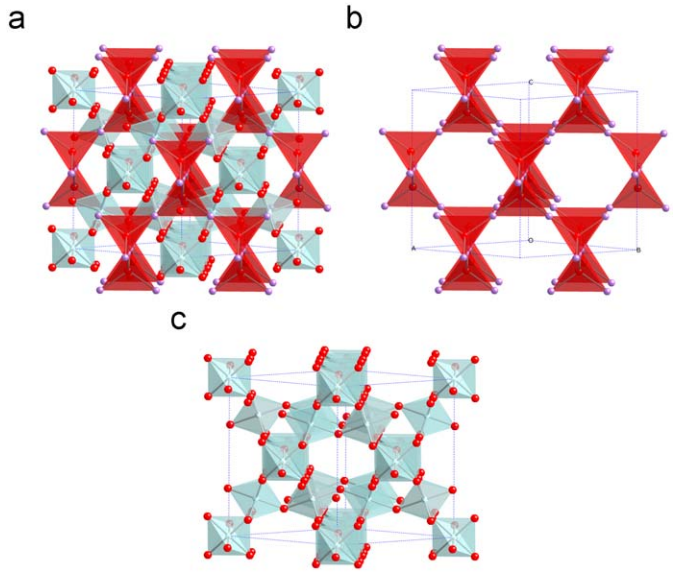

Fig. 1. The (a) ideal $A_2B_2O_6O'$ pyrochlore structure combines the (b) A_2O' network of corner sharing A_4O' tetrahedrons and (c) the B_2O_6 network of corner sharing BO_6 octahedrons.

have been synthesized with S on the O′ site [4,12] the goal of this study is not to detail stable pyrochlore compounds with sulfur substitutions. Instead we take a purely theoretical approach to provide further insight into the lone pair formation in $Bi_2Ti_2O'O_6$. Sulfur may substitute onto either of the two sites occupied by oxygen, which are the 8*b* (X′) site within the A_2O' network and 48*f* (X) site within the B_2O_6 network. We create three configurations with sulfur substituted (i) only on the 8*b* (X′) site, (ii) only the 48*f* (X) site and (iii) on both the 8*b* (X′) and 48*f* (X) sites with the molecular formulas of $Bi_2Ti_2S'O_6$, $Bi_2Ti_2O'S_6$ and $Bi_2Ti_2S'S_6$, respectively. We find that S substitution only on the O′ site can suppress cation displacement, confirming the primary importance of the Bi–O′ interactions. Comparisons of the electronic structure shows that the S substitution on the O′ site modifies the Bi-anion hybridization which suppresses the formation of the lone pair. We also show by examining S substitution on the B_2O_6 network of $Bi_2Ru_2O_6O'$ that cation displacement and lone pair formation can be induced in the metallic Bi pyrochlores by disrupting the Bi–O interactions.

2. Calculation details

First-principles calculations were performed with Vienna *Ab-initio* Simulation Package (VASP) [13–16], a plane-wave DFT code, using the projector augmented wave (PAW) pseudopotentials provided in the VASP database [17,18]. We include the Bi(5*d*, 6*s*, 6*p*), Ti(3*s*, 3*p*, 3*d*, 4*s*), O(2*s*, 2*p*), and/or S(3*s*, 3*p*) orbitals as the valence electrons. The DFT calculations were performed within the local density approximation (LDA) [19]. The LDA is expected to underestimate lattice constants and overestimate the strength of bonding, but has been found to be more accurate than the GGA functionals for many metal oxides [20,21]. We tested the generalized gradient approximation (GGA) with the parameterization of Perdew et al. [22] for a series of Bi-based pyrochlores and showed qualitative agreement with the LDA results reported [5]. We have confirmed the favorability of atomic displacement or lone pair formation does not depend on the functionals. Electronic relaxation was performed with the conjugate gradient (CG) method accelerated using Methfessel-Paxton Fermi-level smearing with a Gaussian width of 0.1 eV [23]. All calculations were performed at fixed volume and shape, while the atoms were relaxed until the forces were less than 0.03 eV/Å. Though all atoms are free to relax in these optimized structures the crystal lattice is fixed to the cubic pyrochlore structure. This restriction was tested in our previous study of Bi pyrochlores [5]. A plane wave cutoff energy of 400 eV was used along with a $3\times3\times3$ Monkhorst-Pack [24] mesh, resulting in 14 irreducible *k*-points. Test calculations done with 450 eV cutoff and a $4\times4\times4$ mesh resulted in differences less than 0.01 eV/88-atom unit cell in the total energy, well within the error for the results presented in this paper.

To probe minima associated with displaced cations, we performed simulated annealing calculations under fixed crystal shape and volume using *ab initio* molecular dynamics (MD) [13–16] with the relaxed ideal pyrochlore structures (from the above procedure) as the initial structures. The MD simulations were conducted with only the Γ point within the NVT ensemble starting at 1000 K and cooling to 300 K over 500 MD steps with a time step of 0.5 fs. After MD simulation, the system was minimized using the same approach as outlined above ($3\times3\times3$ mesh, CG method, etc.) and the equilibrium lattice parameter was reevaluated for the cation displaced structure. While the MD simulation is over extremely short times, we confirmed increasing the simulation length does not affect the final fully relaxed structure.

3. Results and discussion

3.1. Structural details

For each of the bismuth pyrochlores ($Bi_2Ti_2X'X_6$, *X*=O or S) we determine the equilibrium lattice parameter by generating energy versus volume curves. Table 1 contains the equilibrium lattice parameters for the $Bi_2Ti_2O'O_6$, $Bi_2Ti_2S'O_6$, $Bi_2Ti_2O'S_6$ and $Bi_2Ti_2S'S_6$ pyrochlore system. Though there is no experimental data available for comparison in the sulfur containing systems, in the $Bi_2Ti_2O'O_6$ system there is excellent agreement between our DFT value of 10.34 Å and the experimental values of 10.357 Å for $Bi_{1.74}Ti_2O_{6.62}$ [7] and 10.35907 Å for $Bi_2Ti_2O_7$ [6]. In our earlier study, DFT predicted lattice parameters for other Bi-based pyrochlores were within 1% of experimental values providing confidence in DFT's ability to reproduce these structures [5].

$Bi_2Ti_2S'O_6$ has only 8 sulfur atoms per unit cell and shows the smallest lattice expansion from 10.23 to 10.65 Å. When the number of sulfur atoms is increased to 48 per unit cell in the $Bi_2Ti_2O'S_6$, a much larger lattice expansion to 12.0 Å is observed. In the $Bi_2Ti_2S'S_6$, with sulfur on both the X′ (8*b*) and X (48*f*) sites, the lattice expands slightly more to an equilibrium lattice parameter of 12.3 Å. It is well known that S anions are larger than O anions so the lattice expansion is not unexpected. In order to understand if the lattice expansion depended only on the incorporation of the larger sulfur anion on various lattice sites, we identified the real space volume occupied by each atom within the lattice. Utilizing the code of Henkelman et al. [25], we determined the Bader volumes based on the Bader criteria for decomposing the electron density [26]. Since the Bader volumes are calculated using the zero-flux surfaces in the electron density gradient, the sum of Bader volumes in a crystal will exactly equal the total cell volume. Therefore, each Bader volume will depend on the equilibrium lattice volume. To compare the atomic volume of an atom on a specific site between the various crystal systems examined, we scaled each Bader volume by its corresponding total unit cell volume. As expected, we found the scaled Bader volume of the Ti cation and O anion remain the same between the $Bi_2Ti_2O'O_6$ and the $Bi_2Ti_2S'O_6$ system. However, the scaled Bader volume of the Bi cation was reduced by 8% while the S increased

Table 1
The cubic lattice parameter in Å and average bond lengths in Å of the ideal structure (before annealing) is shown for the $Bi_2Ti_2X'X_6$ and $Bi_2Ru_2O'X_6$ pyrochlore systems.

	Lattice parameter (Å)	Expansion percentage (%)	Bond length (Å)			Bond expansion percentage (%)		
			Bi–X′	Bi–X	B–X	Bi–X′	Bi–X	B–X
$Bi_2Ti_2O'O_6$	10.23	–	2.21	2.55	1.96	–	–	–
$Bi_2Ti_2S'O_6$	10.65	4.1	2.31	2.69	2.02	4.5	5.5	3.1
$Bi_2Ti_2O'S_6$	12.00	17.3	2.59	2.91	2.35	17.2	14.1	19.9
$Bi_2Ti_2S'S_6$	12.30	20.2	2.66	3.03	2.38	20.4	18.8	21.4
$Bi_2Ru_2O'O_6$	10.205	–	2.21	2.51	1.98	–	–	–
$Bi_2Ru_2O'S_6$	11.75	15.1	2.54	2.88	2.28	15.1	14.8	15.2

Table 2
The cubic lattice parameter in Å, energy change in eV/Bi atom, and average displacement magnitudes in Å after simulated annealing with respect to the ideal structure with positive energy indicating an increase in thermodynamic favorability are shown for the $Bi_2Ti_2O'O_6$, $Bi_2Ti_2S'O_6$, $Bi_2Ti_2O'S_6$, and $Bi_2Ru_2O'S_6$ pyrochlore systems.

	Lattice parameter (Å)	Energy change (eV/Bi)	Displacement magnitude (Å) [Scaled by lattice parameter (Å/Å)]			Bond length (Å)		
			Bi	B	X′	Bi–X′	Bi–X	B–X
$Bi_2Ti_2O'O_6$	10.34	0.146 ± 0.001	0.38 ± 0.02 $[0.037 \pm 0.002]$	0.07 ± 0.02 $[0.007 \pm 0.002]$	0.11 ± 0.01 $[0.011 \pm 0.001]$	2.26 ± 0.04	2.34 ± 0.11	1.96 ± 0.05
$Bi_2Ti_2S'O_6$	10.65	0.000	0.00 ± 0.00 $[0.000 \pm 0.000]$	0.01 ± 0.00 $[0.001 \pm 0.000]$	0.00 ± 0.00 $[0.000 \pm 0.000]$	2.31 ± 0.00	2.69 ± 0.00	2.02 ± 0.00
$Bi_2Ti_2O'S_6$	12.00	0.533	0.51 ± 0.14 $[0.043 \pm 0.012]$	0.40 ± 0.14 $[0.034 \pm 0.012]$	0.71 ± 0.18 $[0.059 \pm 0.015]$	2.33 ± 0.27	2.85 ± 0.14	2.39 ± 0.08
$Bi_2Ru_2O'S_6$	11.75	0.064	0.23 ± 0.03 $[0.019 \pm 0.002]$	0.01 ± 0.00 $[0.001 \pm 0.000]$	0.20 ± 0.00 $[0.017 \pm 0.000]$	2.56 ± 0.35	2.89 ± 0.04	2.28 ± 0.01

The average bond lengths are provided in Å.

the X′ (8*b*) site volume by 23%. In the $Bi_2Ti_2O'S_6$ system the S anion increased the X (48*f*) site volume by 15% in comparison to the $Bi_2Ti_2O'O_6$ system. Between the $Bi_2Ti_2O'O_6$ and the $Bi_2Ti_2O'S_6$ systems, the Bi, Ti, and O′ atoms showed volume reductions of 27%, 24%, and 27%, respectively. Based on the variations in the Bader volumes we conclude the equilibrium lattice parameter may not be determined *a priori* with only the atomic volumes of the constituent atoms.

Table 1 also shows the Bi–X′, Bi–X, and B–X bond lengths, where X can represent either O or S atom. As expected, the lattice expansion increases all the bond lengths significantly. In the ideal pyrochlore structure only the O atom experiences non-zero forces and will undergo atomic relaxation to optimize both the Bi–O and Ti–O bond lengths. Therefore, the Bi–X′ bond length scales directly with the lattice parameter. Some variations are observed when the bond lengths corresponding to the O site are examined. In the $Bi_2Ti_2S'O_6$ system, there is a 4.1% lattice expansion but the Ti–O bond only increases by 3.1%. This smaller Ti–O bond length indicates the Ti atom bonds more strongly to the O atoms and therefore pulls the O atoms in closer, which then elongates the Bi–O bond by 5.5%. In both the $Bi_2Ti_2O'S_6$ and $Bi_2Ti_2S'S_6$ systems, the Bi–S bond is reduced with respect to the lattice expansion and the Ti–S bond is elongated, indicating the Bi–S interactions are stronger than the Ti–S interactions.

We probe for atomic displacement in our three materials by performing simulated annealing as discussed in Section 2, with the results summarized in Table 2. Since the lattice parameters vary considerably between the systems, both the average displacement magnitudes and these magnitudes scaled by the equilibrium lattice parameter are included in Table 2. In $Bi_2Ti_2S'O_6$, atomic displacement is not favored since we observe no significant energy change or atomic displacement. Additionally, we attempted to forcibly push the Bi cations out of the ideal 16*d* site and after atomic relaxation we observed $Bi_2Ti_2S'O_6$ does not retain the pyrochlore structure. The resulting structure is not energetically favorable with respect to the undisplaced pyrochlore structure; therefore, the ideal pyrochlore structure without cation displacement is taken as the preferred structure for the $Bi_2Ti_2S'O_6$ system.

Alternatively, atomic displacement is favored in the $Bi_2Ti_2O'S_6$ system with an energy change of 0.53 eV per Bi cation. When comparing this value with that reported in the $Bi_2Ti_2O'O_6$ system of 0.15 eV per Bi cation [5], the atomic displacement here is 3.5 times more favorable. This larger preference for the displaced structure is attributed to the disruption of the Bi–Ti_2O_6 interactions. The Bi cation interacts less with the Ti_2S_6 network than the Ti_2O_6 network, which in turn allows for stronger Bi–O′ hybridization. As we will discuss in more detail in Section 3.2, the Bi–O′ interactions leads to lone pair formation and corresponding atomic displacement. For $Bi_2Ti_2O'S_6$, these stronger Bi–O′ interactions make the asymmetric atomic displaced structure much more favorable over the ideal structure with no cation displacement. In the $Bi_2Ti_2O'O_6$ system the Bi cation displaces on average 0.38 Å and in $Bi_2Ti_2O'S_6$ the Bi cations are displacing on average 0.51 Å. Additionally, in $Bi_2Ti_2O'S_6$ the 0.7 Å atomic displacement of the Ti atoms is more than four times that seen in the $Bi_2Ti_2O'O_6$ system. The average bond lengths are included in Table 2. The Bi displacement in the $Bi_2Ti_2O'S_6$ system reduces the Bi–O′ bond length from 2.59 to 2.33 Å and is comparable to the 2.26 Å bond length of $Bi_2Ti_2O'O_6$. Table 2 shows the averaged Ti–S bond length is not significantly altered by the large displacement of Ti. However, within each of the Ti centered octahedron there are variations in the six local Ti–S bonds with up to a 0.2 Å variance of the Ti–S bond lengths within some of the octahedrons.

Though the results are not included, the simulated annealing of $Bi_2Ti_2S'S_6$ shows similar results to $Bi_2Ti_2S'O_6$ with minimal atomic displacement observed initially and lattice distortion upon forcible atomic displacement. Since atomic displacement in $Bi_2Ti_2O'O_6$ can be suppressed by S substitution on the O′ site, the $Bi_2Ti_2S'S_6$ system is redundant and convolutes the role of the

A_2O' and B_2O_6 networks and therefore will be excluded from the following discussion.

3.2. Electronic structure

The results presented in Section 3.1 clearly indicate that S substitution on the A_2O' network is needed to suppress cation displacement. This section will focus on understanding the differences in the electronic structures between the $Bi_2Ti_2S'O_6$ and $Bi_2Ti_2O'S_6$ systems and how these systems relate to the $Bi_2Ti_2O'O_6$ pyrochlore both before and after atomic displacement. The electron localization function (ELF) introduced by Becke and Edgecombe [27] provides a simple real space technique of mapping electrons into core, shell, bonding, and lone pair electrons based on the Pauli exclusion principle. The technique has been advanced by Savin and Silvi in an effort to provide a more quantitative description of the chemical bond [28,29]. The ELF function maps the probable distribution of electrons graphically, where a fully localized (delocalized) electron has an ELF value of 1 (0). We use the ELF function below to identify active lone pair formation on the Bi cations as a function of S substitution on the X (48*f*) and X′ (8*b*) sites.

The ELF is plotted in Fig. 2 for the $Bi_2Ti_2O'O_6$ pyrochlore after atomic displacement in the (110) plane intersecting the Bi–O and Ti–O bonding environment. After simulated annealing, the Bi cation displaces to the right with an asymmetric lobe of increased electron localization forming to the left of the Bi cation in the vacant space. It is through the development of this asymmetric lone pair that atomic displacement is favored in the $Bi_2Ti_2O'O_6$ system. To understand why atomic displacement is not observed in the $Bi_2Ti_2S'O_6$ system we examine the electronic structure for this system with the same atomic displacement as that seen in the $Bi_2Ti_2O'O_6$ pyrochlore without allowing atomic relaxation. The ELF for the $Bi_2Ti_2S'O_6$ pyrochlore with forced displacement is plotted in Fig. 3 in the same (110) plane. Though the Bi cation in the center of Fig. 3 is displaced in the same fashion as that in Fig. 2, the electron localization observed in Fig. 3 surrounding the Bi cation shows negligible asymmetry character, indicating a p-type lone pair does not form in this system. In fact, the ELF for the $Bi_2Ti_2S'O_6$ system more closely resembles the symmetric localization previously reported for $Bi_2Ti_2O'O_6$ pyrochlore without atomic displacement on the A_2O' network [30]. In the earlier study the observed symmetric lobes are due to site symmetry with the Bi and O′ in their ideal 16*d* and 8*b* crystallographic sites and are termed a s-type lone pair. In our systems, it is interesting to note within the same atomic structure (i.e. displacement

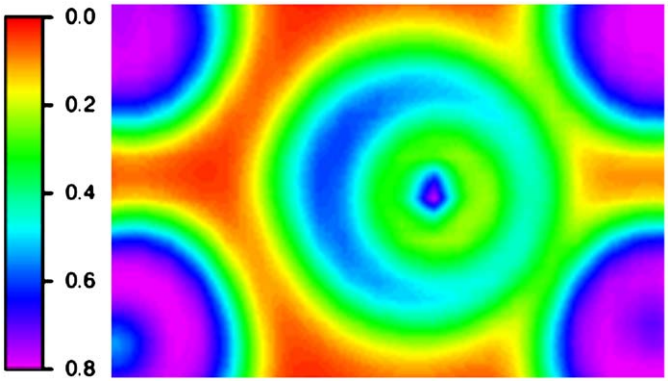

Fig. 2. The electron localization of the $Bi_2Ti_2O'O_6$ with atomic displacement for part of the (110) plane passing through one Bi atom (center) and four O ions (in the corners). The ELF values range from 0.0 (red) to 0.8 (purple) as indicated by the scale. (For interpretation of the references to color in this figure legend, the reader is referred to the web version of this article.)

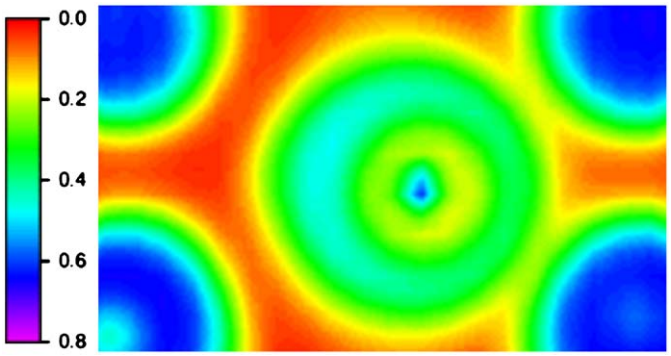

Fig. 3. The electron localization of the $Bi_2Ti_2S'O_6$ with forced atomic displacement for part of the (110) plane passing through one Bi atom (center) and four O ions (in the corners). The ELF values range from 0.0 (red) to 0.8 (purple) as indicated by the scale. (For interpretation of the references to color in this figure legend, the reader is referred to the web version of this article.)

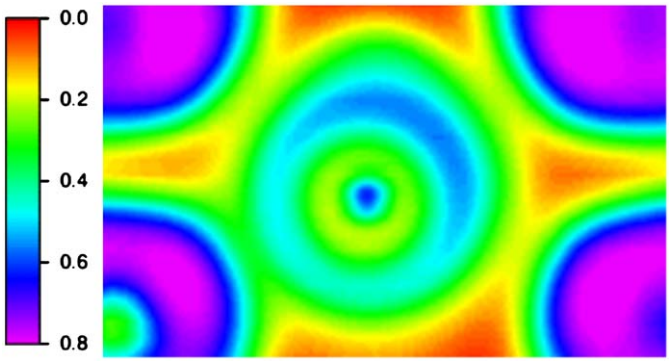

Fig. 4. The electron localization of the $Bi_2Ti_2O'S_6$ with atomic displacement for part of the (110) plane passing through one Bi atom (center) and four S ions (in the corners). The ELF values range from 0.0 (red) to 0.8 (purple) as indicated by the scale. (For interpretation of the references to color in this figure legend, the reader is referred to the web version of this article.)

pattern) that Bi–O′ interactions lead to atomic displacement and an asymmetric p-type electron localization for $Bi_2Ti_2O'O_6$ while Bi–S′ suppresses p-type electron localization for $Bi_2Ti_2S'O_6$. Fig. 4 illustrates the ELF plotted in the same (110) plane for the $Bi_2Ti_2O'S_6$ pyrochlore after simulated annealing. It is clear the atomic displacement in this system does not exactly match that observed in the $Bi_2Ti_2O'O_6$ pyrochlore but surrounding the Bi cation is an asymmetric lone pair. Therefore the development of a p-type lone pair on the Bi cation is observed in the two pyrochlores with favorable atomic displacement and not observed in the pyrochlore with forced atomic displacement. The effect of S substitution onto the X′ site on the p-type lone pair formation is explored in more detail in the discussion of partial density of states (pDOS) below.

To quantify charge transfer in these systems we determined the Bader atomic charges [26] using the code of Henkelman et al. [25]. The Bader charges for the most favored structure, i.e. either with or without displacement, of each of the pyrochlore systems examined are included in Table 3. The importance of covalency can be seen in these systems since all ions deviate from their formal charge values. Wang et al. [31] addressed covalent versus ionic bonding in bismuth pyrochlore using differences in the ion electronegativity. Ionic (covalent) bonding would dominate with the larger (smaller) difference in electronegativity between the two bonded atoms. In our earlier study, the Bi–O bonds were identified to be more ionic in nature than the B–O bonds in metallic pyrochlores (*B*=Ru, Os, Ir, and Rh). Inversely, for $Bi_2Ti_2O_7$,

the Bi–O bonds are more covalent in nature than the Ti–O bonds. These observations suggest that to observe cation displacement and p-type lone pair formation we need to either increase the strength of the Bi–O′ interactions or weaken the B–O interactions. As we show below this simple rule is not sufficient to describe the behavior of Bi pyrochlores upon S substitution.

The Bader charges for both the ideal and S substituted $Bi_2Ti_2O_7$ pyrochlores are reported in Table 3. These Bader values may be interpreted in conjunction with the changes to the electronegativity differences upon sulfur substitution. With increasing sulfur content, the Bi Bader charge decreases from 1.88 e for $Bi_2Ti_2O'O_6$ to 1.63 e for $Bi_2Ti_2S'O_6$ to 1.47 e for $Bi_2Ti_2O'S_6$, indicating the degree of covalent bonding is increasing with increasing sulfur content. Using Pauling's [32] electronegativity (EN) for Bi, Ti, and O, in $Bi_2Ti_2O'O_6$ the difference in EN between Bi and O is 1.42 while the difference between Ti and O is 1.9. In $Bi_2Ti_2S'O_6$, the difference in EN between Bi and S is 0.56 significantly lower than the Ti–O; therefore, the Bi–S′ bond should be more covalent than the Ti–O bond. Table 3 shows the Bader charges of Bi and S′ are significantly less than their respective formal charges and that the Ti and O charges do not change between $Bi_2Ti_2O'O_6$ and $Bi_2Ti_2S'O_6$. With sulfur occupying the X site, the difference in EN between Ti and S is 1.04, between Bi and O′ is 1.42 and between Bi and S is 0.56. We can predict the Bi–O′ bond should be more ionic than the Bi–S bond which should be more ionic than the Ti–S bond. The calculated Bader charges again agree with this prediction with reduction of the Bi, Ti, O′ and S charges. While the Bader charges reflect the changes in covalency expected from using the differences in EN, they fail to predict the systems were cation displacement occurs. For example, the Bi cation becomes more covalent as we go from $Bi_2Ti_2O'O_6$, $Bi_2Ti_2S'O_6$, and $Bi_2Ti_2O'S_6$ but only the two end systems show atomic displacement. While $Bi_2Ti_2S'O_6$ shows larger charge transfer between the Bi and X′ than in the $Bi_2Ti_2O'O_6$ system, it is only the latter that produces a strong p-type lone pair and atomic displacement. As we discuss below cation displacement and lone pair formation are dictated by the nature of the Bi–X′ hybridization, which is distinctly different in the $Bi_2Ti_2O'O_6$ and $Bi_2Ti_2S'O_6$ systems.

Fig. 5 compares the pDOS determined for the previously reported $Bi_2Ti_2O'O_6$ [5] (a–d) before and (e–h) after atomic displacement, with the states separated for each atom type.

Table 3
Bader atomic charges in units of e for the Bi, B, X′, and X atoms are shown for the $Bi_2Ti_2O'O_6$, $Bi_2Ti_2S'O_6$, $Bi_2Ti_2O'S_6$, $Bi_2Ru_2O'O_6$, and $Bi_2Ru_2O'S_6$ pyrochlore systems.

	Lattice parameter (Å)	Bader charge (*e*)			
		Bi	B	X′	X
$Bi_2Ti_2O'O_6$[a]	10.34	1.88	2.18	−1.22	−1.15
$Bi_2Ti_2S'O_6$	10.65	1.63	2.21	−0.81	−1.15
$Bi_2Ti_2O'S_6$[a]	12.00	1.47	1.62	−1.14	−0.84
$Bi_2Ru_2O'O_6$	10.205	1.90	1.61	−1.27	−0.96
$Bi_2Ru_2O'S_6$[a]	11.75	1.37	0.66	−1.13	−0.49

[a] Indicates systems that prefer atomic displacements.

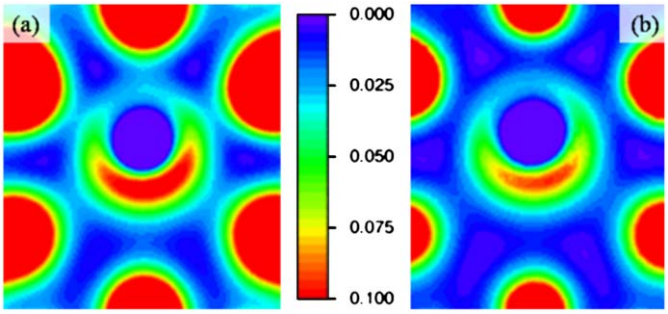

Fig. 6. The partial electron densities for the (a) $Bi_2Ti_2O'O_6$ with atomic displacement and (b) $Bi_2Ti_2S'O_6$ with forced atomic displacement for the states between −2 eV to the Fermi level for part of the (111) plane passing through one Bi atom (center) and six O ions (edges) with the scale indicating the contour levels between 0.0 (blue) and 0.1 e/Å^3 (red). (For interpretation of the references to color in this figure legend, the reader is referred to the web version of this article.)

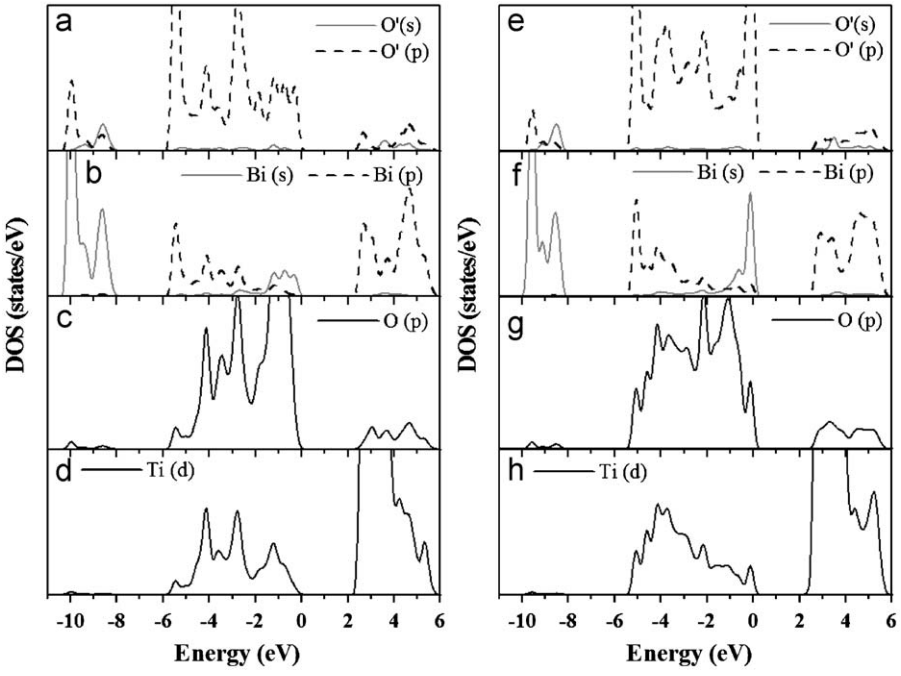

Fig. 5. Partial density of states of O′ 2*s*, O′ 2*p*, Bi 6*s*, Bi 6*p*, O 2*p*, and Ti 3*d* in states per electron volt for the $Bi_2Ti_2O_7$ pyrochlore at 10.23 Å (a–d) before and (e–h) after atomic displacement and volume expansion to 10.34 Å.

Figs. 5a and e compare the O′2*s* and 2*p* states before and after displacement, respectively. At the low energy band corresponding to the Bi 6*s* states (see Fig. 5b and f), there is considerable hybridization between the O′ 2*s* and 2*p* states to overlap with the Bi 6*s* orbital. Additionally, displacement significantly alters the valence band near the Fermi level with increased hybridization of the Bi 6*s* and 6*p* states and improves the overlap with the O′ 2*p* orbital. The central features of the pDOS responsible for lone pair formation can be identified by examining the partial electron density at specific energy windows. We have examined the partial electron density for the low energy band (−11 to −8 eV), the intermediate energy band (−6 to −2 eV) and the top of the valence band (−2 eV to the Fermi level). The energy range at the top of the valence band shows the most clear asymmetric electron density and can be attributed with the lone pair with the Bi 6*s* and 6*p* orbitals strongly overlapping with the O′ 2*p* orbital in the $Bi_2Ti_2O'O_6$ displaced system (see Fig. 5f). Fig. 6 shows the partial electron density for $Bi_2Ti_2O'O_6$ (Fig. 6a) with atomic displacement and $Bi_2Ti_2S'O_6$ (Fig. 6b) with forced atomic displacement. The planes illustrated in Fig. 6 correspond to a Bi cation, in the center of the plane, displaced upward and surrounded by its six O anions. Similar to Fig. 2, the lone pair on the Bi cation can be observed in the opposite direction of the displacement. In both cases, an asymmetric lobe is formed but the size and magnitude of density are much smaller in $Bi_2Ti_2S'O_6$ (Fig. 6b) than in $Bi_2Ti_2O'O_6$ (Fig. 6a), agreeing with the observations made from the ELF that lone pair formation is not favored for $Bi_2Ti_2S'O_6$ (Fig. 3).

Fig. 7 shows the pDOS for the $Bi_2Ti_2S'O_6$ pyrochlore (a–d) at equilibrium and (e–h) with forced atomic displacement. The forced displacement system is the same structure mentioned above with regards to Fig. 3. Although $Bi_2Ti_2S'O_6$ is insulating like $Bi_2Ti_2O'O_6$ (Fig. 5), the magnitude of the band gap has been reduced from 1.8 to 1.5 eV. The pDOS associated with the S′ site, shown in Fig. 7a, shows the 3*s* and 3*p* states directly overlap in the low energy band corresponding to the Bi 6*s* states (see Fig. 7b) which differs from that observed for O′ in $Bi_2Ti_2O'O_6$ (Fig. 5a and e). In the upper valence band, the S′ 3*p* states are considerably lower in energy than equivalent O′ states resulting in a peak split of the Bi 6*p* at the low energy range of this band. This split results in a small energy window where only the Bi 6*p* orbital interacts with the S′ 3*p* orbital, which is not observed in any other pyrochlore. After forced displacement (Fig. 7e–f), this interaction is shifted in energy towards the other interactions within the upper valence band. Additionally, the direct overlap of the S′ 3*s* and 3*p* states seen in the low energy valence band is reduced and mirrors that observed for $Bi_2Ti_2O'O_6$ (Fig. 5a and e). While there is an increase in hybridization of the Bi 6*s* and 6*p* (Fig. 7f) near the Fermi level after forced displacement its magnitude is much smaller than that seen in $Bi_2Ti_2O'O_6$ (Fig. 5f). This corresponds to the previous observation of the symmetric electron localization (Fig. 3) surrounding the Bi cations within this structure.

Fig. 8 compares the pDOS for $Bi_2Ti_2O'S_6$ (a–d) before and (e–h) after atomic displacement. In the $Bi_2Ti_2O'S_6$ system, the band gap between the conducting and valence band is not observed but the energy gap between the two valence bands is retained. The O′ 2*s* and 2*p* states (Fig. 8e) in the lower valence band overlap with the Bi 6*s* states (Fig. 8f) at the higher and lower energy, respectively. This hybridization matches that seen for $Bi_2Ti_2O'O_6$ (Fig. 5e–f). In the upper valence band, atomic displacement significantly increases the overlap of the Bi 6*s* and 6*p* orbitals near the Fermi level (see Fig. 8f) with the O′ 2*p* states (see Fig. 8e), corresponding to the formation of the lone pair observed in Fig. 4. The essential interactions between Bi 6*s* and O′ states at the low energy band and subsequent hybridization between the Bi 6*p* near the Fermi level that mediate the forming of the lone pair in $Bi_2Ti_2O'O_6$ is similar to the findings of Walsh and co-workers for a range of oxides [8–11].

3.3. Bismuth ruthenate

We concluded our study by returning to a representative metallic bismuth pyrochlore, $Bi_2Ru_2O_6O'$, that in our earlier DFT

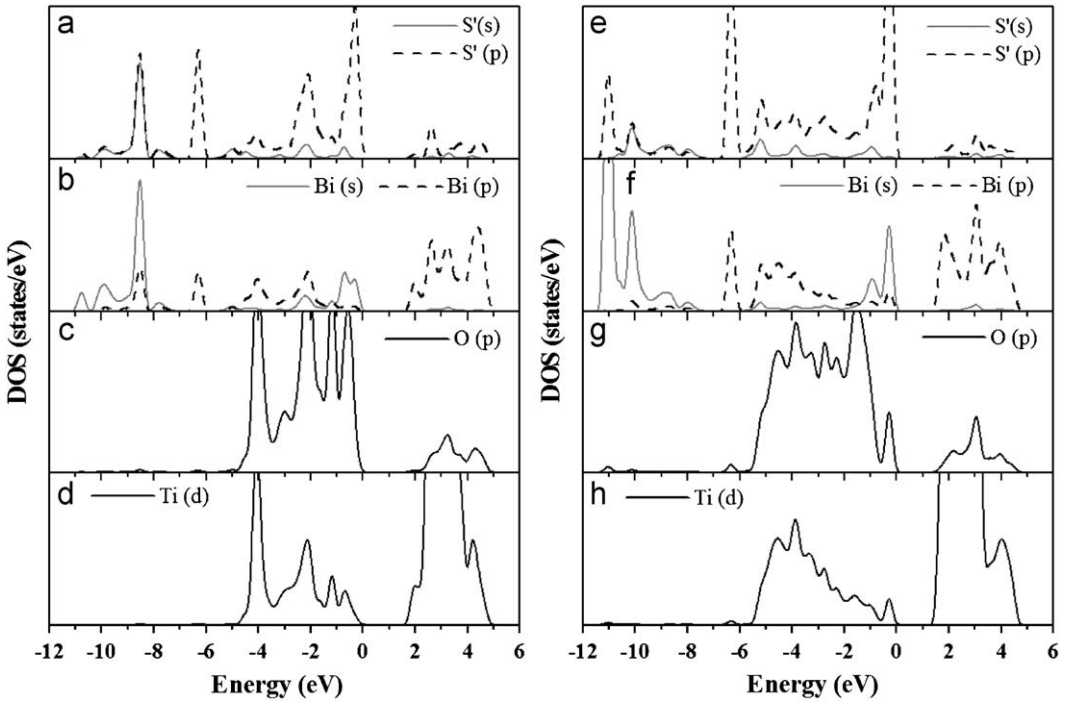

Fig. 7. Partial density of states of S′ 3*s*, S′ 3*p*, Bi 6*s*, Bi 6*p*, O 2*p*, and Ti 3*d* in states per electron volt for the $Bi_2Ti_2S'O_6$ pyrochlore at 10.65 Å (a–d) before and (e–h) after forced atomic displacement.

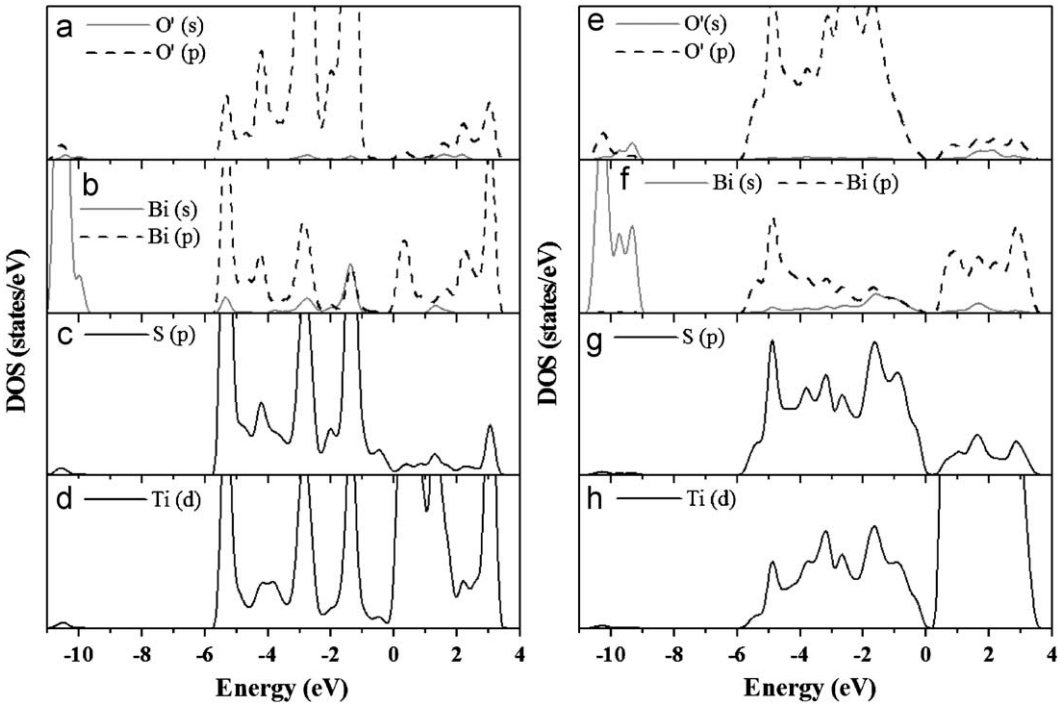

Fig. 8. Partial density of states of O′ 2*s*, O′ 2*p*, Bi 6*s*, Bi 6*p*, S 3*p*, and Ti 3*d* in states per electron volt for the $Bi_2Ti_2O'S_6$ pyrochlore at 12.0 Å (a–d) before and (e–h) after atomic displacement.

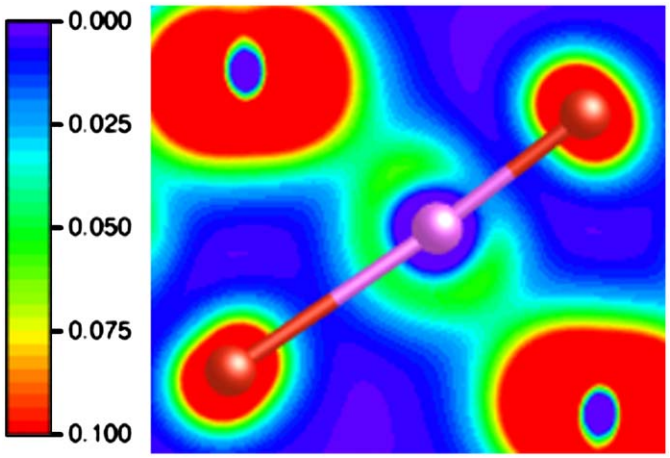

Fig. 9. The partial electron densities for $Bi_2Ru_2O'S_6$ with atomic displacement for the states between −2 eV to the Fermi level for part of the $(\bar{1}\,0\,1)$ plane passing through one Bi atom (center), two O′ (atoms included) and two S ions with the scale indicating the contour levels between 0.0 (blue) and 0.1 e/Å^3 (red). (For interpretation of the references to color in this figure legend, the reader is referred to the web version of this article.)

study did not show any cation displacement [5]. Experimental studies of $Bi_2Ru_2O_6O'$ showed atomic displacement [33], but the samples had significant oxygen deficiency on the A_2O' network. This oxygen deficiency might force the experimentally observed displacement and disagreement with DFT [5], but we leave the study of O vacancies on cation displacement for future studies. In our earlier study [5] on metallic Bi pyrochlores we concluded atomic displacement is not favored due to the stronger interactions between Bi and the O atoms on the B_2O_6 network in these systems. For $Bi_2Ti_2O_6O'$ the cation displacement is enhanced and the p-type lone pair formation more pronounced when S is substituted in the B_2O_6 network. This result suggests that substituting sulfur in the B_2O_6 network for the metallic pyrochlores may induce cation displacement. Below we test this hypothesis by examining sulfur substitution on $Bi_2Ru_2O_6O'$.

We repeated the lattice optimization procedure discussed in Section 3.1 for the $Bi_2Ru_2O'S_6$ structure to determine the equilibrium lattice parameter and favorability of atomic displacement. The structural details of the ideal pyrochlore both with and without sulfur are included in Table 1. Following simulated annealing, we found that atomic displacement is favored in the $Bi_2Ru_2O'S_6$ pyrochlore, with the details summarized in Table 2. The Bi cations in the $Bi_2Ru_2O'S_6$ pyrochlore displace towards one of the two O′ anions thereby creating two long and two short Bi–O′ bonds within each A_4O' tetrahedral (see Fig. 1b). In other bismuth based pyrochlores, this type of Bi cation displacement has been discussed as "spin-ice" tetrahedral bonding [30]. The pyrochlore O′ anions are equated to oxygen within ice with two hydrogen ions covalently bonded and two hydrogen ions more weakly bound at significantly longer distances. While the spin-ice arrangement does not affect the average Bi–O′ bond in the pyrochlore, structurally a single long and short Bi–O′ bond can be seen by looking at the atoms included in Fig. 9. In addition to showing some structural details, Fig. 9 illustrates the partial electron density for a portion of the $(\bar{1}\,0\,1)$, which slices through the S–Bi–O′ bonding network. The energy range of interest, −2 eV to the Fermi energy, is the same as that examined in the $Bi_2Ti_2O_7$ pyrochlore (Fig. 6). A similar asymmetric electron density to that seen in the $Bi_2Ti_2O_7$ is observed for the $Bi_2Ru_2O'S_6$ pyrochlore after atomic displacement, but the electron density maximum is larger (0.1 e/Å^3 versus 0.05 e/Å^3) in $Bi_2Ti_2O_7$. Fig. 10 shows the ELF for $Bi_2Ru_2O'S_6$ with atomic displacement in the $(\bar{1}\,0\,1)$ plane and illustrates an asymmetric lobe forms along the long Bi–O′ bond direction created behind the Bi cation displacement. Though the magnitude of electron localization in $Bi_2Ru_2O'S_6$ (Fig. 10) is lower than that seen in $Bi_2Ti_2O'O_6$ (Fig. 2), we can see in $Bi_2Ru_2O'S_6$ the lone pair formation is favored and triggers the atomic

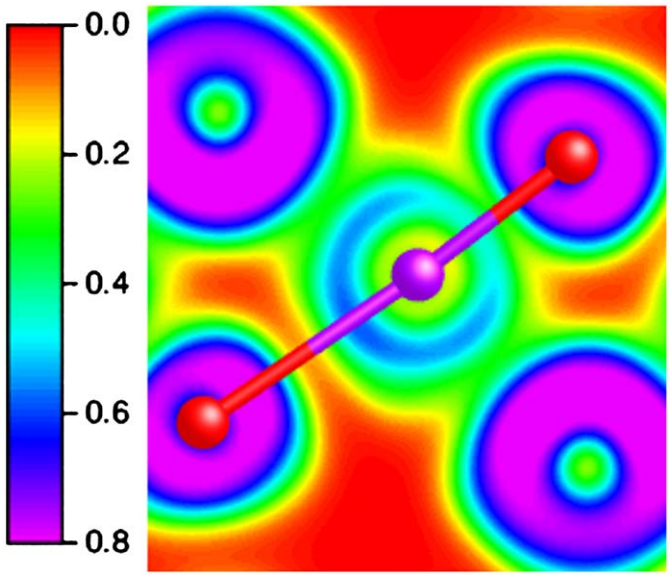

Fig. 10. The electron localization function for $Bi_2Ru_2O'S_6$ with atomic displacement for part of the $(\bar{1}\,0\,1)$ plane passing through one Bi atom (center), two O′ (atoms included) and two S ions. The ELF values range from 0.0 (red) to 0.8 (purple) as indicated by the scale. (For interpretation of the references to color in this figure legend, the reader is referred to the web version of this article.)

displacement. The Bader charges for the $Bi_2Ru_2O'O_6$ and $Bi_2Ru_2O'S_6$ systems are reported at the bottom of Table 3. Similar to the bismuth titanate systems, sulfur incorporation increases the degree of covalent bonding in the system, as indicated by the reduction of the Bi, Ru, O′ and O/S site Bader charges.

These results suggest that modifying the B_2O_6 network to weaken Bi–O interactions is a plausible strategy to increase cation displacement and in turn induce favorable dielectric properties in these materials. It will be interesting to compare the lone pair formation and role in cation displacement in the more complex Bi pyrochlores such as BZN to our observations of $Bi_2Ti_2O_7$.

4. Conclusions

In this paper, we employ DFT calculations to further clarify the lone pair formation in $Bi_2Ti_2O'O_6$ through sulfur substitution on the O′ and O sites. We find atomic displacement is not favored in the case of S substituted on the O′ site, confirming the primary importance of the Bi–O′ interactions. Analysis of the partial density of states, ELF and partial electron density shows that the S substitution on the O′ site suppresses the formation of the lone pair by modifying the Bi-anion hybridization. We also examined the electronic structure of the $Bi_2Ti_2S'O_6$ pyrochlore fixed with the same displacement pattern as that seen in $Bi_2Ti_2O'O_6$. In $Bi_2Ti_2S'O_6$ with forced displacement the ELF displayed symmetric lobe around the bismuth cations with a significant reduction of the asymmetric electron density in the energy range of -2 eV to the Fermi level. In the case of sulfur on the O site, atomic displacement is significantly favored energetically in $Bi_2Ti_2O'S_6$ and showed the largest atomic displacement magnitudes. Specifically, the Ti and O′ atoms displaced considerably more in $Bi_2Ti_2O'S_6$ than in $Bi_2Ti_2O'O_6$ which we attribute to weaker Bi–S versus Bi–O interactions that leads to stronger hybridization between the Bi and O′ states that favors the lone pair formation. Finally, we show by substituting S on the B_2O_6 network of $Bi_2Ru_2O'O_6$ that cation displacement and lone pair formation can be induced in the metallic Bi pyrochlores by disrupting the Bi–O interactions. This result suggests that modifying the B_2O_6 network to reduce the interactions with the A_2O' network will assist in promoting cation displacement.

Acknowledgments

We thank Simon Phillpot and Susan Sinnott for helpful discussions. We acknowledge the University of Florida High-Performance Computing Center (http://hpc.ufl.edu) for providing computational resources.

References

[1] I. Levin, T.G. Amos, J.C. Nino, T.A. Vanderah, C.A. Randall, M.T. Lanagan, J. Solid State Chem. 168 (2002) 69–75.
[2] S. Kamba, V. Porokhonskyy, A. Pashkin, V. Bovtun, J. Petzelt, J.C. Nino, S. Trolier-McKinstry, M.T. Lanagan, C.A. Randall, Phys. Rev. B 66 (2002) 054106.
[3] R.L. Withers, T.R. Welberry, A.K. Larsson, Y. Liu, L. Noren, H. Rundlof, F.J. Brink, J. Solid State Chem. 177 (2004) 231–244.
[4] M.A. Subramanian, G. Aravamudan, G.V. Subba Rao, Prog. Solid State Chem. 15 (1983) 55–143.
[5] B.B. Hinojosa, J.C. Nino, A. Asthagiri, Phys. Rev. B 77 (2008) 104123.
[6] A.L. Hector, S.B. Wiggin, J. Solid State Chem. 177 (2004) 139–145.
[7] I. Radosavljevic, J.S.O. Evans, A.W. Sleight, J. Solid State Chem. 136 (1998) 63–66.
[8] A. Walsh, G.W. Watson, J. Solid State Chem. 178 (2005) 1422–1428.
[9] G.W. Watson, S.C. Parker, J. Phys. Chem. B 103 (1999) 1258–1262.
[10] G.W. Watson, S.C. Parker, G. Kresse, Phys. Rev. B 59 (1999) 8481–8486.
[11] A. Walsh, G.W. Watson, D.J. Payne, R.G. Edgell, J.H. Guo, P.A. Glans, T. Learmonth, K.E. Smith, Phys. Rev. B 73 (2006) 235104.
[12] D. Bernard, J. Pannetie, J.Y. Moisan, J. Lucas, J. Solid State Chem. 8 (1973) 31–36.
[13] G. Kresse, J. Furthmuller, Comput. Mater. Sci. 6 (1996) 15–50.
[14] G. Kresse, J. Furthmüller, Phys. Rev. B 54 (1996) 11169.
[15] G. Kresse, J. Hafner, Phys. Rev. B 47 (1993) 558.
[16] G. Kresse, J. Hafner, Phys. Rev. B 49 (1994) 14251.
[17] P.E. Blöchl, Phys. Rev. B 50 (1994) 17953.
[18] G. Kresse, D. Joubert, Phys. Rev. B 59 (1999) 1758.
[19] W. Kohn, L.J. Sham, Phys. Rev. 140 (1965) A1133.
[20] Z.G. Wu, R.E. Cohen, D.J. Singh, Phys. Rev. B 70 (2004) 104112.
[21] Z.G. Wu, R.E. Cohen, Phys. Rev. B 73 (2006) 235116.
[22] J.P. Perdew, K. Burke, M. Ernzerhof, Phys. Rev. Lett. 77 (1996) 3865–3868.
[23] M. Methfessel, A.T. Paxton, Phys. Rev. B 40 (1989) 3616–3621.
[24] H.J. Monkhorst, J.D. Pack, Phys. Rev. B 13 (1976) 5188.
[25] G. Henkelman, A. Arnaldsson, H. Jonsson, Comput. Mater. Sci. 36 (2006) 354–360.
[26] R. Bader, Atoms in Molecules: A Quantum Theory, Oxford University Press, New York, 1990.
[27] A.D. Becke, K.E. Edgecombe, J. Chem. Phys. 92 (1990) 5397–5403.
[28] B. Silvi, A. Savin, Nature 371 (1994) 683–686.
[29] A. Savin, B. Silvi, F. Colonna, Can. J. Chem.-Rev. Can. Chim. 74 (1996) 1088–1096.
[30] R. Seshadri, Solid State Sciences. 8 (2006) 259–266.
[31] X.L. Wang, H. Wang, X. Yao, J. Am. Ceram. Soc. 80 (1997) 2745–2748.
[32] L. Pauling, J. Am. Chem. Soc. 54 (1932) 3570–3582.
[33] M. Avdeev, M.K. Haas, J.D. Jorgensen, R.J. Cava, J. Solid State Chem. 169 (2002) 24–34.